ELSEVIER

Tectonophysics 236 (1994) 201–216

TECTONOPHYSICS

Seismic structure of the uppermost mantle beneath the Kenya rift

G.R. Keller [a], James Mechie [b,1], L.W. Braile [c], W.D. Mooney [d], Claus Prodehl [b]

[a] *Department of Geological Sciences, The University of Texas at El Paso, El Paso, TX 79968-0555, USA*
[b] *Geophysikalisches Institut, Universität Karlsruhe, Hertzstrasse 16, D-76187, Germany*
[c] *Department of Geosciences, Purdue University, West Lafayette, IN 47807, USA*
[d] *U.S. Geological Survey, Office of Earthquake Research, MS 977, 345 Middlefield Road, Menlo Park, CA 94025, USA*

Received 30 June 1992; accepted 8 November 1993

Abstract

A major goal of the Kenya Rift International Seismic Project (KRISP) 1990 experiment was the determination of deep lithospheric structure. In the refraction/wide-angle reflection part of the KRISP effort, the experiment was designed to obtain arrivals to distances in excess of 400 km. Phases from interfaces within the mantle were recorded from many shotpoints, and by design, the best data were obtained along the axial profile. Reflected arrivals from two thin (< 10 km), high-velocity layers were observed along this profile and a refracted arrival was observed from the upper high-velocity layer. These mantle phases were observed on record sections from four axial profile shotpoints so overlapping and reversed coverage was obtained. Both high-velocity layers are deepest beneath Lake Turkana and become more shallow southward as the apex of the Kenya dome is approached. The first layer has a velocity of 8.05–8.15 km/s, is at a depth of about 45 km beneath Lake Turkana, and is observed at depths of about 40 km to the south before it disappears near the base of the crust. The deeper layer has velocities ranging from 7.7 to 7.8 km/s in the south to about 8.3 km/s in the north, has a similar dip as the upper one, and is found at depths of 60–65 km. Mantle arrivals outside the rift valley appear to correlate with this layer. The large amounts of extrusive volcanics associated with the rift suggest compositional anomalies as an explanation for the observed velocity structure. However, the effects of the large heat anomaly associated with the rift indicate that composition alone cannot explain the high-velocity layers observed. These layers require some anisotropy probably due to the preferred orientation of olivine crystals. The seismic model is consistent with hot mantle material rising beneath the Kenya dome in the southern Kenya rift and north-dipping shearing along the rift axis near the base of the lithosphere beneath the northern Kenya rift. This implies lithosphere thickening towards the north and is consistent with a thermal thinning of the lithosphere from below in the south changing to thinning of the lithosphere due to stretching in the north.

1. Introduction

1.1. The crust versus the lithosphere

Beginning in 1981, the International Lithosphere Program began to focus the attention of the international geoscience community on the

Present address: GeoForschungsZentrum, Telegrafenberg A3, D-14407 Potsdam, Germany.

SSDI 0040-1951(94)00031-4

fact that, to fully understand the evolution of the Earth, we need to attack many problems from the standpoint of the entire lithosphere. Geologists and geophysicists often focus their efforts on the upper crust not because they are myopic but because most data available address primarily upper crustal problems. As depth increases, the amount and resolving power of data decrease and the cost of data acquisition generally increases. Many seismic profiling studies aspire to address the structure of the lithosphere, but in fact are primarily studies of crustal structure because of the difficulty and cost of producing seismic sources which penetrate the mantle. In addition, limits on the number of seismic recording systems available usually force compromises on resolution if the long-offset recordings needed for deep penetration are to be obtained. Until recently, only about 100 portable seismographs could usually be amassed for large-scale experiments. Thus, recording offsets of greater than 500 km required a recording spacing of 5 km or more unless it was possible to detonate multiple large sources. Nuclear test facilities were generally the only place where this was possible. Recordings spaced at 5 km or more are not sufficient to obtain the resolution desired by modern standards which requires recording spacings of about 1 km or less.

Continental rifting is a process which involves the entire lithosphere. Thus, a major goal of the Kenya Rift International Seismic Project (KRISP) is to investigate the structure of the entire lithosphere of the Kenya rift. Our approach in 1990 was two-fold. Firstly, we conducted a program of passive seismic monitoring of teleseisms to provide a regional view of velocity structure to depths of 150–170 km (Achauer et al., 1994; Slack and Davis, 1994). Secondly, we designed our profiling experiment to obtain long-offset data from seismic waves which penetrated well into the upper mantle (50–100 km). This second effort is the focus of this paper.

1.2. Previous long-offset recording efforts

Because of the widespread interest in the structure of the upper mantle, long (> 300 km)-offset seismic profiles have received much recent attention. Interest in the upper mantle is not a new phenomenon (e.g., Ansorge and Mueller, 1973) and a number of long profiles have been recorded beginning in the 1960's. Studies prior to the early 1980's were summarized by Fuchs and Vinnik (1982) and Fuchs et al. (1987). Primarily due to the limited opportunities to record large seismic sources, most early efforts were not reversed and had seismic station spacings measured in tens of kilometers. Thus, the resolution attainable from such studies is limited. Deep Seismic Sounding (DSS) experiments in northern Eurasia (e.g., Ryaboy, 1977; Vinnik and Ryaboy, 1981; Yegorkin and Pavlenkova, 1981) and the FENNOLORA line (Guggisberg et al., 1984; Guggisberg, 1986) are the best examples of very long (> 500 km) profiles with reversed, overlapping coverage and relatively closely spaced recordings. Some more recent studies have provided detailed recordings of mantle phases to distances of more than 300 km by either employing a large repeatable air gun source (BABEL Working Group, 1990, 1991) or a very large number (~ 500) of seismic recording instruments (Pacific to Arizona Crustal Experiment, PACE) (Benz et al., 1990). However, even these results were unreversed limiting their resolution of upper mantle velocity structure.

Within rifts, long profiles which have provided information below depths to which the Pn phase penetrates are few in number. From a 400 km long profile recorded along the Jordan–Dead Sea rift, a refraction from a layer within the uppermost mantle has been identified (Ginzburg et al., 1979). Reflections from a layer within the uppermost mantle have been identified on profiles in the Afar depression (Makris and Ginzburg, 1987) and on profiles near the margins of the Red Sea (Mooney et al., 1985; Prodehl, 1985; Mechie et al., 1986; Rihm et al., 1991). These observations have all been interpreted to be due to deep (45–55 km) high-velocity layers which underlie the uppermost mantle.

2. The KRISP long-offset experiment

The results of the KRISP-85 preliminary refraction experiment indicated that we could have

a unique opportunity to probe the upper mantle of a currently active continental rift in a subsequent experiment. The large lakes in the Kenya rift valley were the reason for this opportunity because they could potentially provide efficient shotpoints and overlapping, long-offset profile coverage. Thus, a major element of the design of the KRISP-90 experiment was long-offset recording primarily along the rift axis. The crustal structure results for the axial seismic profile are presented by Mechie et al. (1994a).

Two shotpoints in Lake Turkana (LTN and LTC), a shotpoint in Lake Baringo (BAR), and a shotpoint in Lake Naivasha (NAI) provided a 500-km-long reversed profile (Fig. 1). By employing about 220 seismic recording systems, two deployments (one north of Lake Baringo and one to the south), and multiple sources (two at each shotpoint), a recording spacing of about 1.5 km was obtained. Seismic stations were deployed up to 130 km south of Lake Naivasha in the hope of recording even longer-offset data. Upper mantle arrivals were recorded to distances of greater than 400 km from LTN and LTC and to about 300 km from BAR and NAI.

The upper mantle arrivals from LTN, LTC, BAR and NAI are shown in Figs. 2 to 5, respectively. Close-ups of the intra-mantle phases are shown in Figs. 6 and 7. The Pn phase (d) can be seen on all of the record sections and is locally

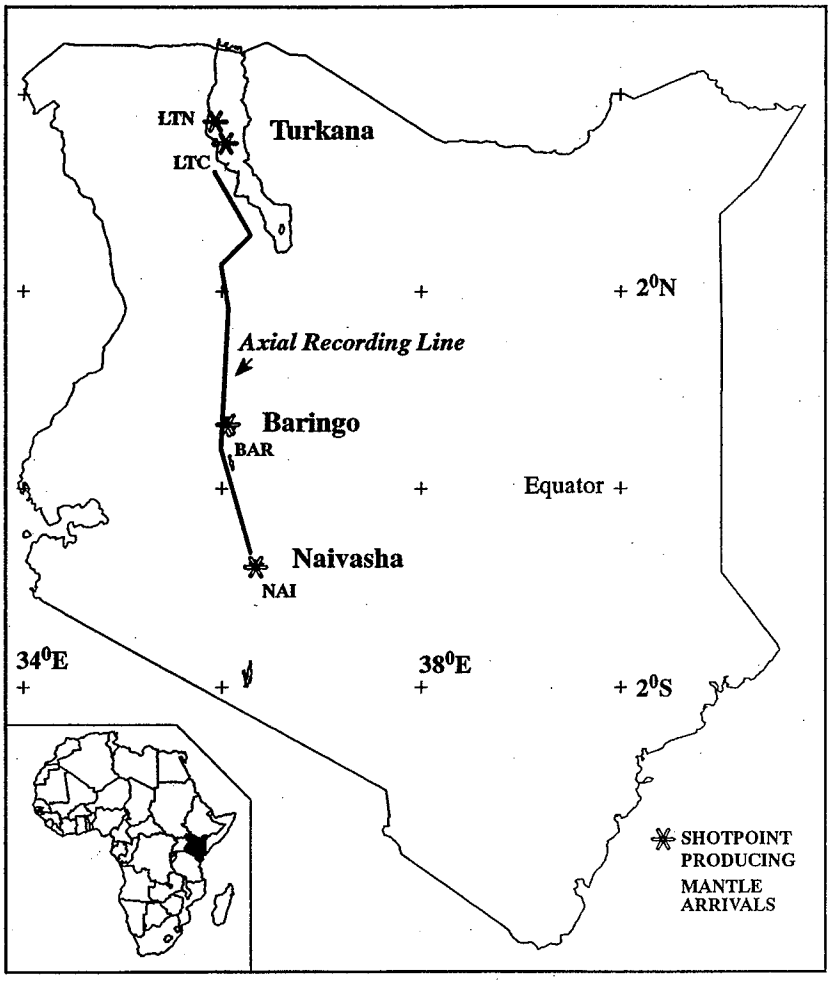

Fig. 1. Index map of the Kenya rift showing shotpoints which produced data on upper mantle structures.

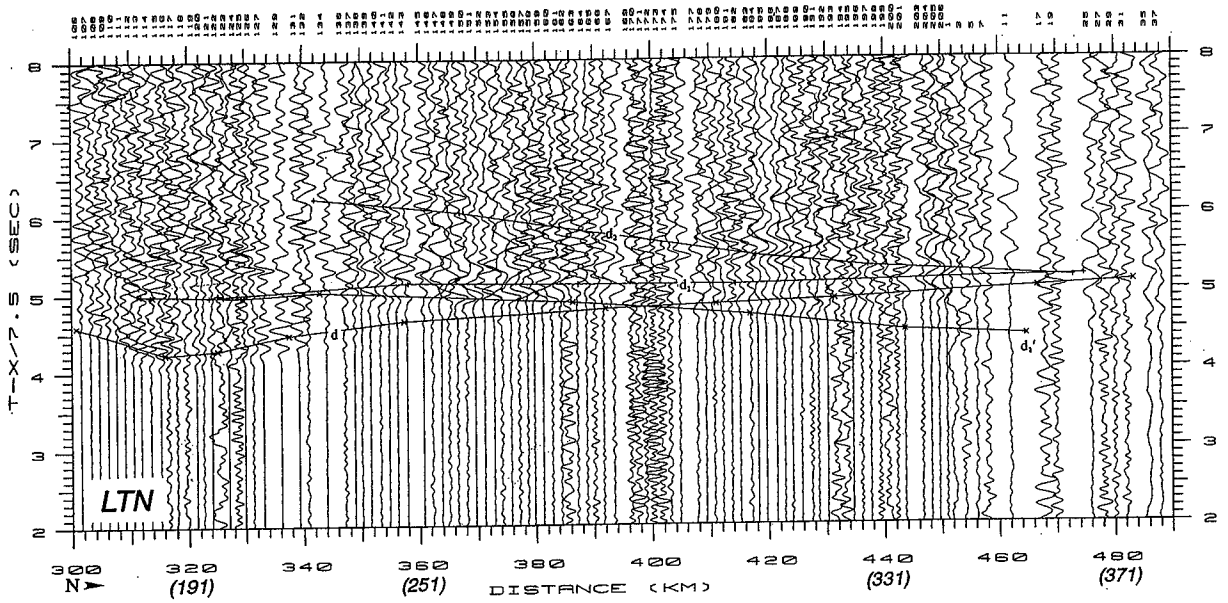

Fig. 2. Record section for the Lake Turkana North (LTN) shotpoint. Reducing velocity 7.5 km/s. Ray-tracing results for the following phases are shown: d (Pn) = refraction from the uppermost mantle; d_1 = reflection from the first upper mantle reflector; d_1' = refraction from the layer beneath the d_1 reflector; d_2 = reflection from the second upper mantle reflector. Distances shown in regular type are in model coordinates. Distances from the shot (shot–receiver offsets) are shown in italics. The shotpoint was at a distance of 109 km.

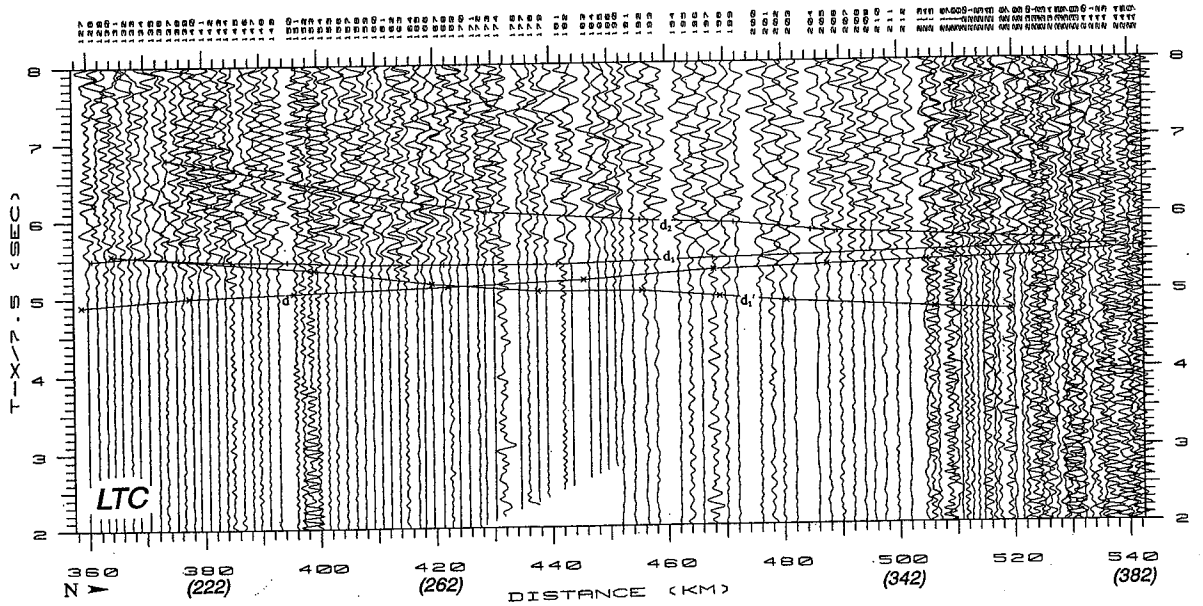

Fig. 3. Record section for the Lake Turkana Central (LTC) shotpoint. Reducing velocity 7.5 km/s. Ray-tracing results for the following phases are shown: d (Pn) = refraction from the uppermost mantle; d_1 = reflection from the first upper mantle reflector; d_1' = refraction from the layer beneath the d_1 reflector; d_2 = reflection from the second upper mantle reflector. Distances shown in regular type are in model coordinates. Distances from the shot (shot–receiver offsets) are shown in italics. The shotpoint was at a distance of 157.5 km.

delayed and advanced significantly by the complex upper crustal structure encountered. Close-ups of this phase are shown in Mechie et al. (1994a). The phase correlations observed would not have been possible without the relatively closely spaced (1–2 km) seismic recordings. It is hard to imagine what the result would have been had the stations been placed 10–20 km apart as has been the case in most previous upper mantle seismic profiles.

When looking at the data for LTN and LTC (Figs. 2, 3, 6), two upper mantle phases, d_1 and d_2, are evident. In addition, on both of these record sections at offsets beyond about 270 and 300 km, respectively, the Pn phase appears to be replaced by a faster phase d_1'. A less prominent reflected mantle phase is also seen on the record sections from BAR and NAI (Figs. 4, 5, 7), and as will be discussed below, is thought to represent d_2 arrivals.

3. Interpretation

The shape of the travel-time curves for the d_1 and d_2 phases on the LTN and LTC record sections implies that they can be considered to be wide-angle reflections from velocity discontinuities below the Moho. Strictly speaking, waves turning in a thin high-velocity-gradient zone could also explain the data at hand. Interpretations of detailed lower lithosphere structure elsewhere (e.g. Kind, 1974; Ansorge, 1975; Cassell and Fuchs, 1979; Burmakov et al., 1987) have revealed thin layers of both high and low velocity. Thus, it was important to determine the polarity of the phases we observed.

From synthetic seismogram modeling we know that if the velocity below a reflector is smaller than that above it, then the reflection has the opposite polarity to the first arrival refraction. However, if the velocity below the reflector is

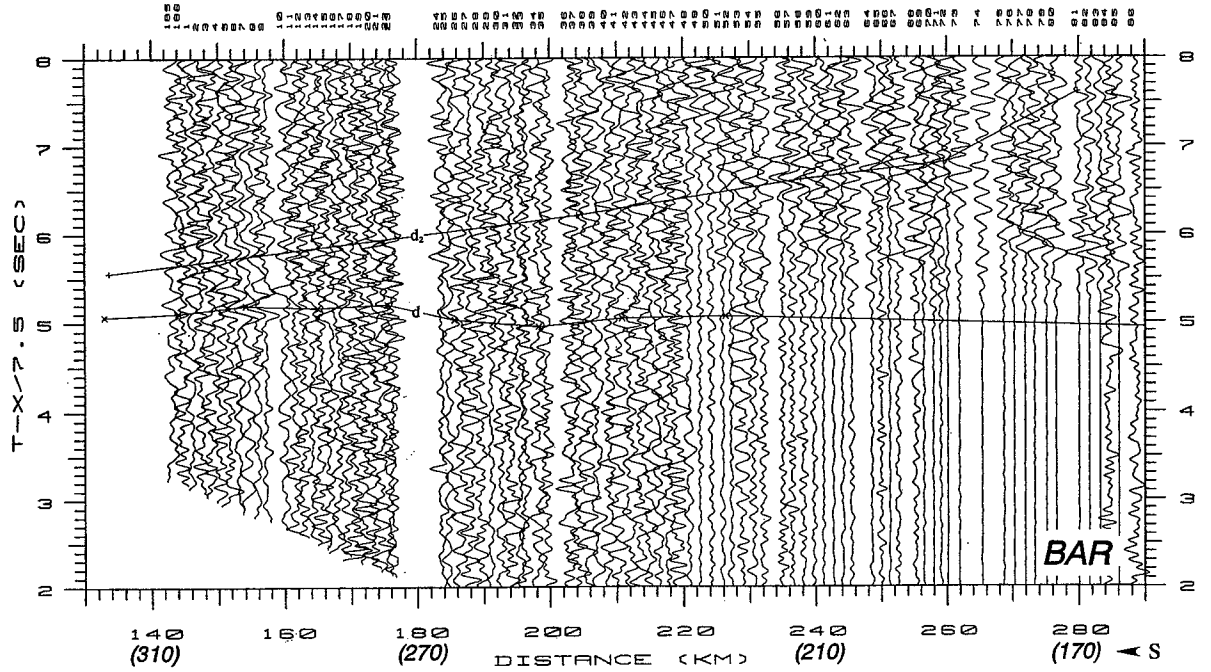

Fig. 4. Record section for the Lake Baringo (BAR) shotpoint. Reducing velocity 7.5 km/s. Ray-tracing results for the following phases are shown: d (Pn) = refraction from the uppermost mantle; d_2 = reflection from the second upper mantle reflector. Distances shown in regular type are in model coordinates. Distances from the shot (shot–receiver offsets) are shown in italics. The shotpoint was at a distance of 450 km.

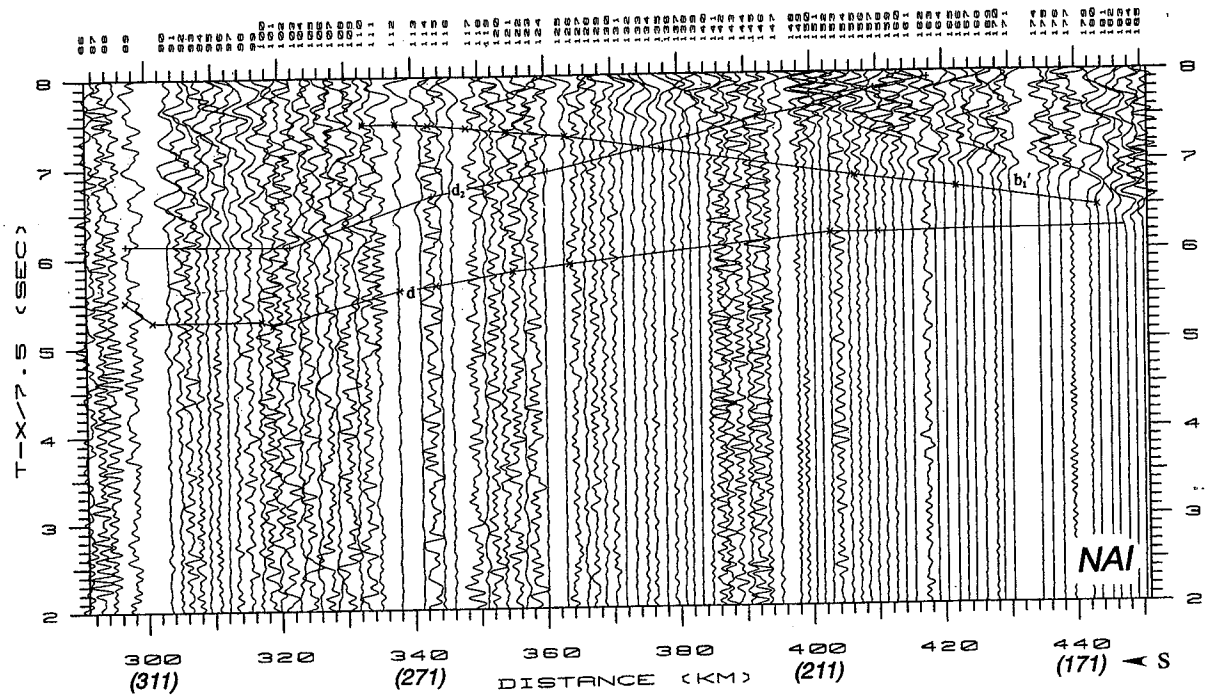

Fig. 5. Record section for the Lake Naivasha (NAI) shotpoint. Reducing velocity 7.5 km/s. Ray-tracing results for the following phases are shown: b_1' = refraction from the top of the 6.8 km/s lower crustal layer; d (Pn) = refraction from the uppermost mantle; d_2 = reflection from the second upper mantle reflector. Distances shown in regular type are in model coordinates. Distances from the shot (shot–receiver offsets) are shown in italics. The shotpoint was at a distance of 611 km.

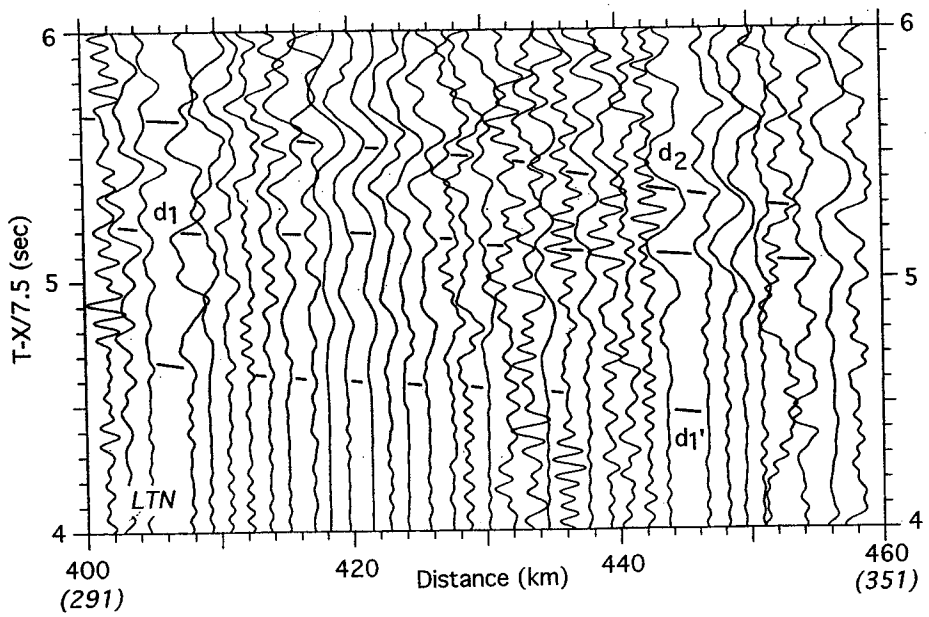

Fig. 6. Close-up of the record section for the mantle phases from LTN. Phases are identified as in Fig. 2. Distances shown in regular type are in model coordinates. Distances from the shot (shot–receiver offsets) are shown in italics.

greater than that above it, then the reflection has the same polarity as the first arrival refraction at a distance less than the critical distance beyond which the phase of the reflection begins to change so that it has opposite polarity to the refraction. Six seismograms from the LTN record section, in the distance range 210–230 km, were stacked for both the Pn (d) and d_1 phases. From a comparison of the stacks (Fig. 8a), it is clear that the polarity of both phases is the same and thus the velocity beneath the reflector is greater than that above it. A similar analysis was carried out for the d'_1 and d_2 phases on the LTN record section. This analysis again showed that both phases have the same polarity, and thus the velocity below the d_2 reflector is greater than that above it (Fig. 8b).

Since the velocity below the d_1 reflector is greater than that above it, it seems reasonable to view the d'_1 phase as the diving wave (head wave) turning in the layer whose top surface produces the d_1 reflected phase. We have no reversals from the south for the d'_1 arrival. However, in order to fit all the travel-time data for both d_1 and d'_1 from LTN and LTC, we require a layer north of BAR with a high true velocity of about 8.1 km/s at a depth of about 45 km beneath LTN and shallowing to the south to about 40 km beneath BAR (Fig. 9).

The high velocities in excess of 8.0 km/s north of BAR pose a dilemma as the teleseismic results indicate that low (< 7.8 km/s) seismic velocities are found to depths of over 150 km beneath the central portion of the rift (Achauer et al., 1994; Slack and Davis, 1994). Although it is true that the refraction and teleseismic results only overlap south of BAR, the gravity model for the axial line (Mechie et al., 1994a) indicates no major density variations in the mantle along the rift. Thus, we feel it is necessary that the velocity model derived from the refraction experiment honors the teleseismic results in an average sense. For this reason, and the fact that at distances in excess of 350 km the d_2 reflection is subparallel to the d'_1 refraction but separated from it by about 0.8 s (Figs. 2, 3, 6), a low-velocity layer was inserted in the northern portion of the model between the two mantle reflectors. Since we also have no information below the d_2 reflector other than the synthetic seismogram modeling of the velocity contrast across it and teleseismic results, we en-

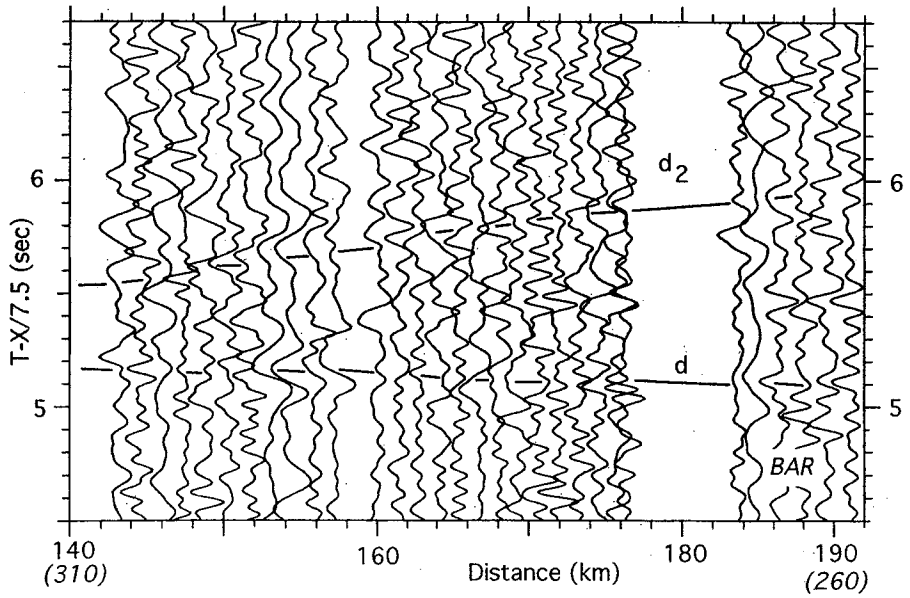

Fig. 7. Close-up of the record section for the mantle phases from BAR. Phases are identified as in Fig. 4. Distances shown in regular type are in model coordinates. Distances from the shot (shot–receiver offsets) are shown in italics.

visage that it is the top of a relatively thin high-velocity layer which is underlain by lower-velocity material.

Only one mantle phase other than Pn (d) was observed on the NAI and BAR record sections. The derived depth for this reflection makes it more likely to correspond to d_2 than to d_1. In fact, the d_1 reflector would intersect the Moho if projected southward beyond BAR. Thus, the d_1 reflector was modeled to die out as it approaches BAR.

The final velocity model derived from ray-trace modeling of LTN, LTC, BAR and NAI data is shown in Fig. 9. The crustal structure and velocities obtained by Mechie et al. (1994a) were honored exactly as were their uppermost mantle velocities. The ray coverage provided by the observed arrivals is depicted in Fig. 10. This diagram helps to illustrate, in a tomographic sense, the constraints actually provided by our data. Velocity–depth functions along the model are shown in Fig. 11.

The velocity model derived was built starting with the crustal model of Mechie et al. (1994a). This part of the model was held fixed throughout the ray-tracing of travel times for the phases which were identified. The choice of these phases is a crucial step in the process whose effect on uncertainty in the final result is hard to estimate. We feel that the evidence for two interfaces in the mantle across which there is a positive velocity contrast is very strong. The correlation between the strong phases observed from Lake Turkana and the weak phase on the records from NAI and BAR is arguable, and it is possible or even likely that the interfaces shown in Figs. 9 and 10 are not continuous. The low-velocity layer was inferred from the need to honor the teleseis-

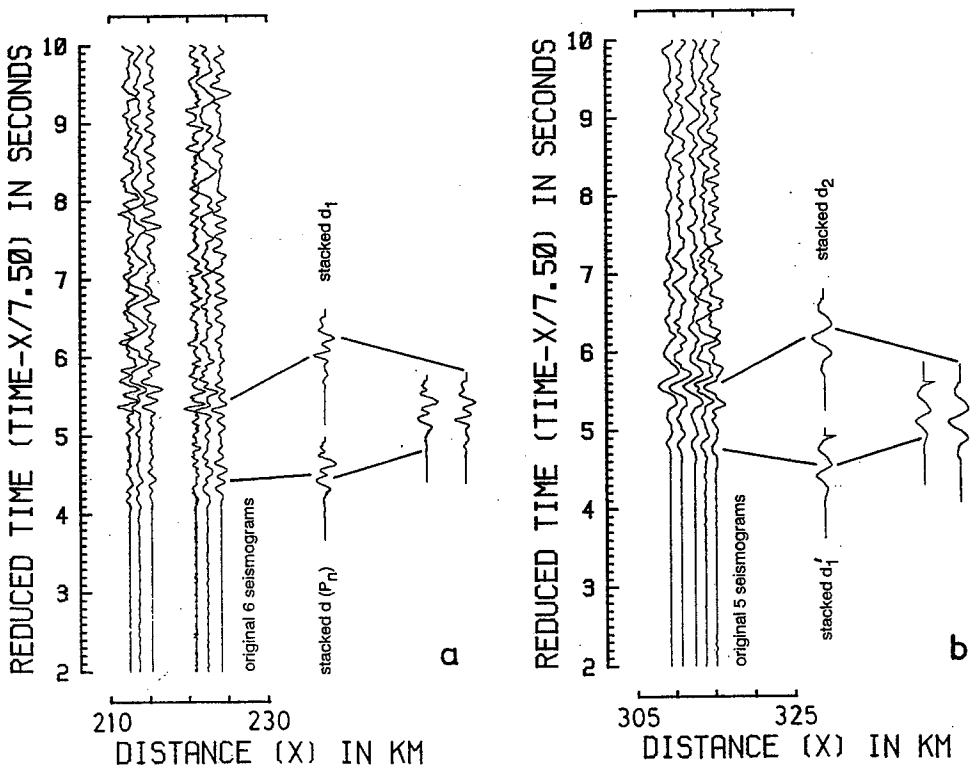

Fig. 8. Seismic records and stacked traces demonstrating polarity relations between reflected and refracted phases. (a) d (Pn) refraction and d_1 reflection. (b) d_1' refraction and d_2 reflection.

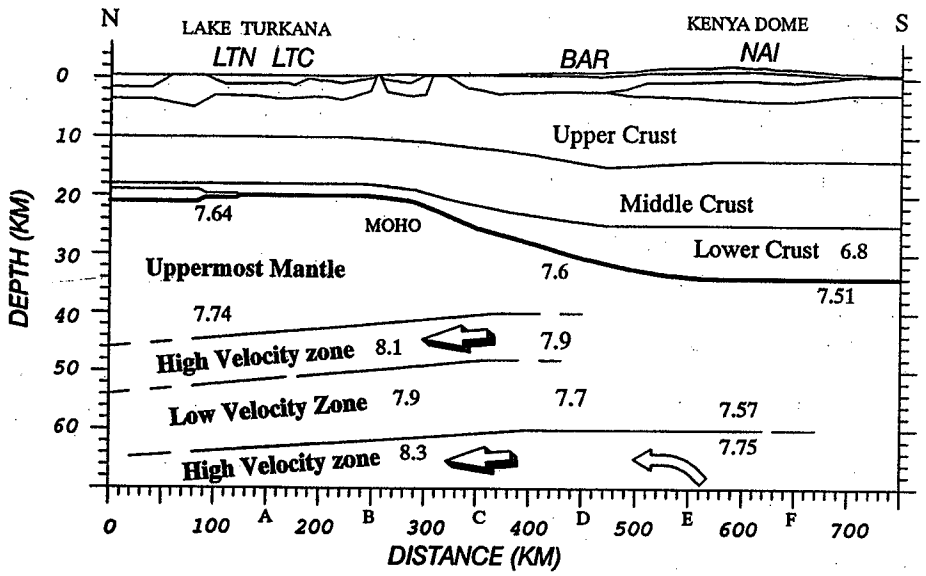

Fig. 9. Velocity model of the axial profile derived from ray-trace and synthetic seismogram modeling. P-wave velocities are indicated in km/s. See Fig. 11 for detailed velocity–depth profiles. Letters indicate positions of these profiles. Arrows indicate envisaged directions of flow possibly caused by shearing.

mic data in an average sense and also from the travel-time delay between the d_2 reflection and the d'_1 refraction at large distances where the two phases are subparallel.

The velocity structure determined from ray-tracing was fine tuned by synthetic seismogram modeling of waveforms. This analysis determined that the first high-velocity layer had to have a

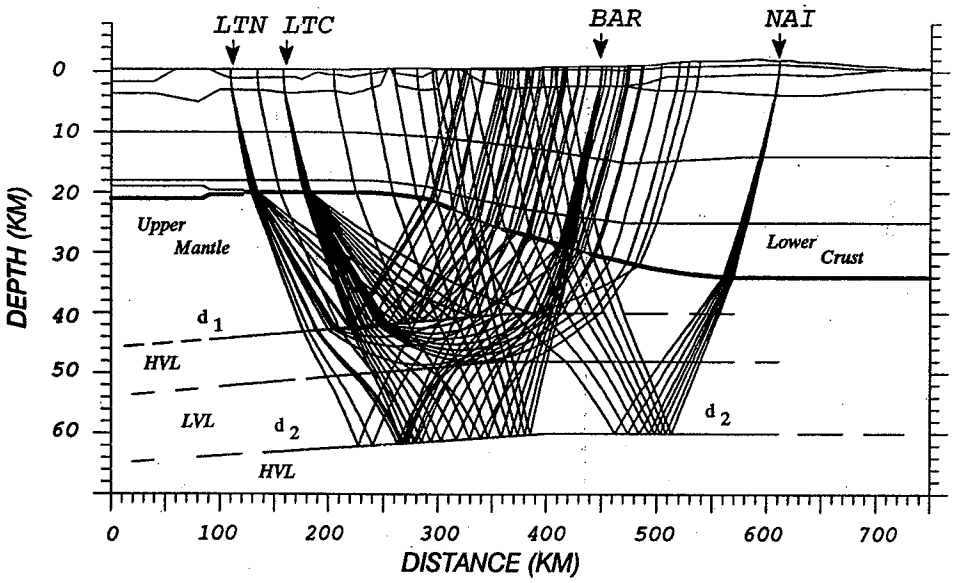

Fig. 10. Ray-tracing diagram showing the ray coverage provided by the observed data. In a general tomographic sense, the coverage indicates the constraints provided by the data. *LVL* = low-velocity layer; *HVL* = high-velocity layer.

minimum thickness of about 8 km and that the velocity contrast across the second interface was much higher in the northern part of the model than beneath the Kenya dome. We calculated synthetic seismograms using the reflectivity method (Fuchs and Müller, 1971) and a finite-differences technique for 2-D heterogeneous media (Kelly et al., 1976; Sandmeier, 1990). The power spectrum of the d'_1 refraction contains a single dominant peak at about 2.5–3.0 Hz, and thus we calculated synthetic seismograms for this frequency range.

A trace-normalized finite-difference synthetic record section for LTN is shown in Fig. 12. The ray-trace model was digitized at a grid spacing of 50 m for the calculations. In the synthetic record section, the amplitudes of the first arrival refractions are small compared to those of the reflected phases, d_1 and d_2, in general agreement with the observed data. The model also produces strong amplitudes for the reflection d_2 beyond about 260 km distance in the synthetic record section. In the observed data, this phase can be best observed beyond 280–300 km distance. In the synthetic record section, the reflection d_1 appears to be too dominant with respect to the first arrival refractions and the reflection d_2. Since the Pn velocity in the layer above the reflector and the velocity in the layer immediately below the reflector are both well constrained by our model, this may indicate that there is some fairly small-scale reflector topography and/or velocity inhomogeneity in the vicinity of the reflector in order to reduce the amplitudes of the reflection d_1 in the observed data.

The amplitude modeling thus indicates that north of BAR, the velocities below the d_2 reflector at depths of 60–65 km are about 8.3 km/s

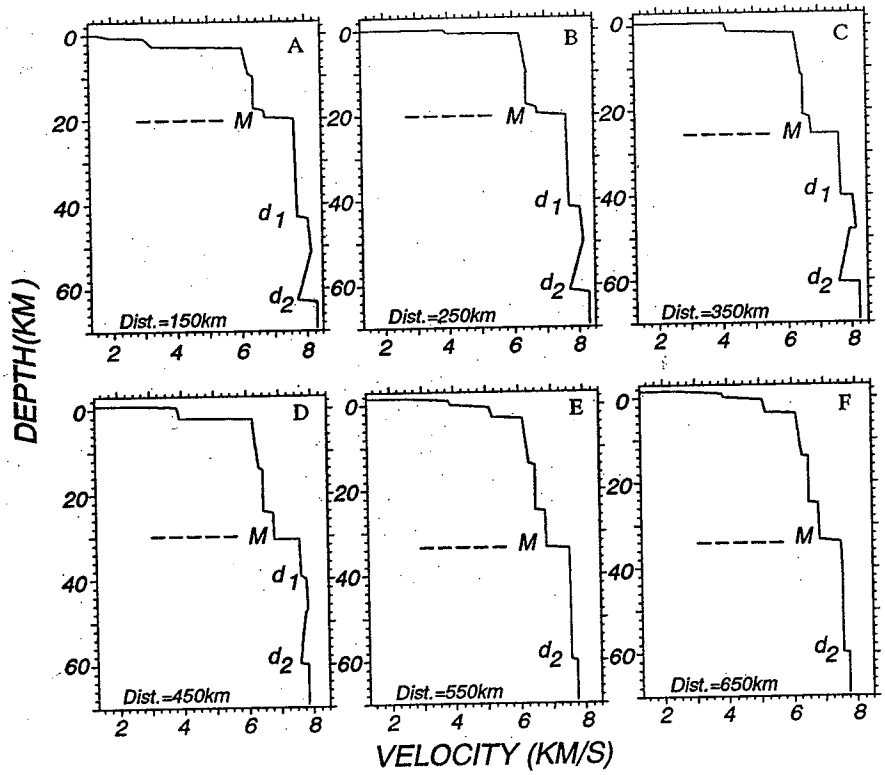

Fig. 11. Velocity–depth profiles at selected locations along the rift valley. Distances for profiles are shown in model coordinates. M = Moho, d_1-first mantle interface, d_2-second mantle interface. Letters refer to locations in Fig. 9.

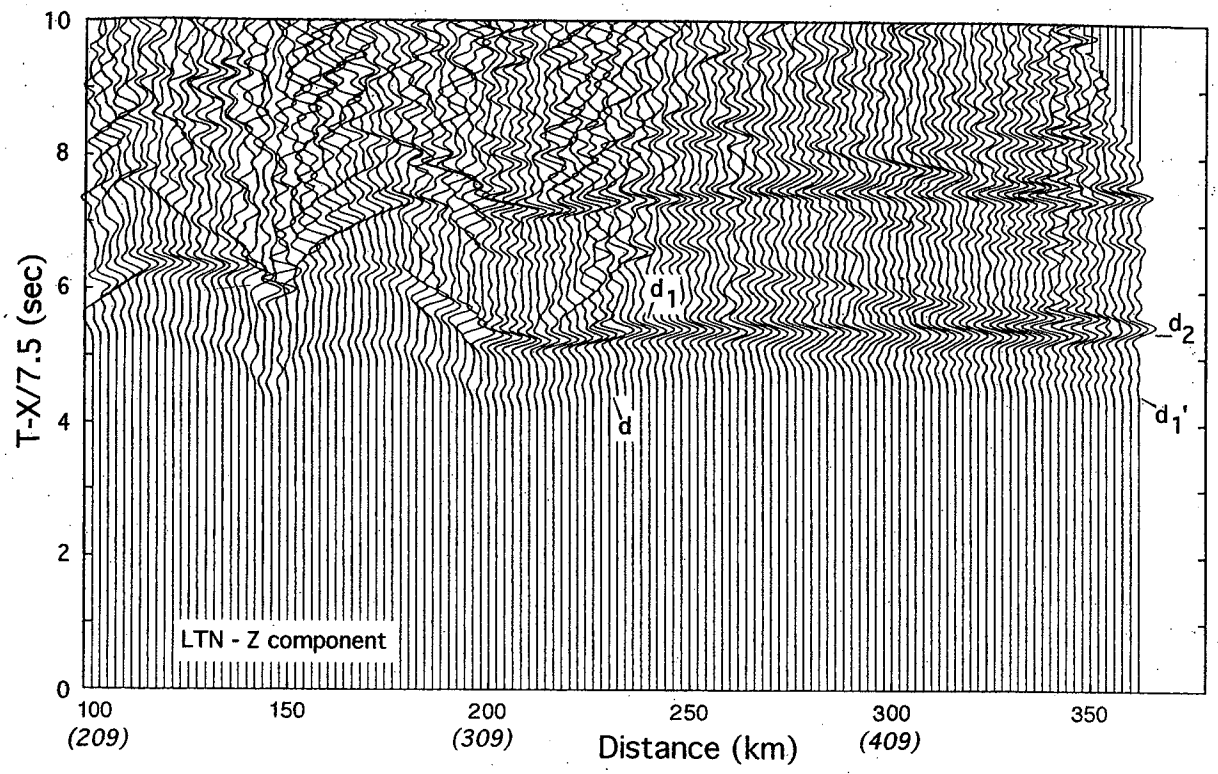

Fig. 12. Synthetic seismograms for the LTN shotpoint calculated by using a finite-differences technique (Sandmeier, 1990).

and that between the two high-velocity layers, the low-velocity layer is about 10 km thick and has an average velocity of about 7.9 km/s. South of BAR, the velocities below the d_2 reflector are considerably lower at about 7.7–7.8 km/s.

The finite-difference synthetics were so time-consuming that it was not feasible to make many iterations on the model with this technique. However, the overall similarity between the synthetics and the actual data significantly increases our confidence in the velocity model. The final result of the integrated modeling process is also consistent with the teleseismic results and gravity anomalies.

4. Discussion

Utilizing polarity, travel-time and amplitude information for long-offset data from the axial line of the KRISP-90 experiment, an interpretation of the uppermost mantle down to 60–70 km depth beneath the axis of the Kenya rift has been derived. The results reveal that north of BAR, in the northern portion of the rift, two upper mantle high-velocity layers separated by a low-velocity zone exist (Figs. 9, 11). The first of these layers, at 40–45 km depth, has a velocity of 8.05–8.15 km/s while the second, at 60–65 km depth, has a velocity of around 8.3 km/s. The layer at 40–45 km depth has a thickness of at least about 8 km while the thickness of the layer at 60–65 km depth could not be determined beyond saying that it only should be a few kilometers thick, so that the teleseismic results can be honored in an average sense. South of BAR, beneath the southern part of the rift, the upper mantle is characterized by velocities of 7.5–7.6 km/s down to about 60 km depth where the velocity increases to about 7.7–7.8 km/s.

The teleseismic results (low mantle velocities) can be readily explained in terms of partial melting of about 5% (Achauer et al., 1994). The areas of low P-wave velocity in the earth model derived here (Fig. 9) can be similarly explained. The

question that remains is the origin of the regions of high (> 8.0 km/s) P-wave velocity. It is hard to imagine any region of the mantle beneath the rift escaping the thermal anomaly associated with the rifting, so we seem left with a compositional effect and/or a preferred mineral orientation (anisotropic) effect to explain the high-velocity layers.

As discussed earlier, layers of alternating high and low velocity have been observed in the mantle in several regions of the world including the cratonal regions of northern Eurasia. Thus, one has to ask if the mantle structures observed here are simply relics of pre-existing structures which do not correlate with the modern rift zone. The geometry of our recording lines is less than ideal to address the question of the lateral extent of the mantle structures to the east and west of the rift valley. However, our shotpoint in Lake Victoria (VIC) was very energetic, and a mantle phase which correlates with the d_2 arrivals from NAI has been identified by Maguire et al. (1994). Ray-tracing of these arrivals indicates that the d_2 reflector extends 50–100 km west of the rift. East of the rift, Prodehl et al. (1994) found evidence for a reflector in the mantle at depths of about 47 km beneath the KRISP-90 flank profile. The reflection correlates with the d_1 arrival described here, and the reflector deepens away from the rift.

These observations are all in areas which have experienced significant rift-related volcanism and which teleseismic and gravity data indicate are underlain by lithosphere disturbed by the rifting process. Thus, we cannot definitely state that the mantle structures defined are not observed beyond the rifted region. However, if one considers that over 100,000 km^3 of volcanics have been erupted in the region traversed by the seismic lines (Williams, 1972; Karson and Curtis, 1989; MacDonald, 1994) and that the plutonic rocks associated with these extrusives would conservatively have a volume on the order of four times greater (Karson and Curtis, 1989), it seems extremely unlikely that older features in the lithospheric mantle would survive to produce the rather continuous structures we have observed. The volume of magmatism does suggest that these mantle structures could be interpreted to be the boundaries of sill-like features which have high velocities because they are the depleted ultramafic plutonic source from which large volumes of mafic magmas were derived. Following the petrologic arguments of Karson and Curtis (1989), we see that one or two sills which are 5–10 km thick and which extend 50–150 km east and west of the rift valley would have volumes on the order of those suggested by Karson and Curtis (1989). To the extent that composition is responsible for the observed velocity variations, sill-like features which have magmatically sourced the surface volcanics seem the best explanation for the observed mantle structures. O'Reilly et al. (1990) show that the magnitude of the velocity variations observed could be reasonably obtained from variations in mantle composition, but as discussed below, temperature effects require more than simple compositional variations to explain the higher velocity values (8.1–8.3 km/s).

Mechie et al. (1994b) have examined the petrologic implications of the upper mantle velocities observed in the KRISP-90 data. At the high temperatures of 950–1100°C which can be expected beneath the rift axis (Morgan, 1983; Macdonald, 1994), even pure olivine rock with no preferred mineral orientation will have a velocity less than 8.05 km/s at 40–45 km depth and less than 8.1 km/s at 60–65 km depth. Thus it seems necessary to have some preferred mineral orientation (anisotropy) to explain the observed high velocities. One possible explanation is that the olivine is oriented so that the slow *b*-axis is vertical, and the faster *a*- and *c*-axes are oriented randomly in the horizontal plane. This produces a transversely isotropic structure with no expected azimuthal dependence of upper mantle velocities in the refraction data. In this model, an undepleted peridotite would produce the required velocities of 8.05–8.15 km/s at 40–45 km depth while a slightly depleted peridotite with around 65% olivine would result in the required velocity of 8.3 km/s at 60–65 km depth. This model makes sense volumetrically and has the advantage that its effect on gravity is small since the absence of partial melt in the high-velocity layers and a maximum increase in olivine by about 10% only

causes a density change of about 0.02 g/cm^3. A further advantage is that with the slow *b*-axis of olivine being vertical, the teleseismic rays which essentially travel vertically through this part of the mantle, will not observe the fast horizontal velocity.

It is also known that mechanisms which cause olivine to show preferred orientation tend to orient the *b*-axis perpendicular to the plane of the flow (Nicolas et al. 1971; N.G. Bussod, pers. commun., 1992). Thus, in the high-velocity mantle layers, we envisage a horizontal flow possibly caused by shearing. Nicolas et al. (1971) also describe the situation in which the flow (shearing) is accompanied by recrystallisation. The two processes working together can yield randomly oriented *a*- and *c*-axes in the plane of the flow (Nicolas et al. 1971). Thus it could be possible that flow perpendicular to the rift axis accompanied by recrystallisation would produce the envisaged transverse isotropic structure.

It should be pointed out at this stage that there are other models which could also explain the high-velocity mantle layers. For example, if all three axes of olivine showed a preferred direction of orientation, then a model with orthorhombic symmetry would result. For such a model to produce velocities high enough to match the observed velocities in the 40–45 km depth range, about 40% of the olivine would have to have the fast *a*-axis oriented horizontally along the rift axis. In the 60–65 km depth range, about 55% of the olivine would have to have the fast *a*-axis similarly oriented. In this case, there would be azimuthal dependence of the upper mantle velocities in the refraction data, and it is envisaged that the flow would be parallel to the rift axis. There would thus be a discrepancy between this situation and that of the oceans where the direction of maximum velocity is perpendicular to the direction of the oceanic ridge (Raitt et al., 1971). It is also different from the situation found in the western USA where the direction of maximum velocity is nearly E–W (Bamford et al., 1979; Hearn, 1984) and thus perpendicular to the nearby East Pacific oceanic ridge. The discrepancy could be explained if hot mantle material is envisaged rising below the Kenya dome in the southern portion of the rift and flow and thus shearing is radially directed away from the center of this hot material. If recrystallisation accompanied this flow, then a transverse isotropic structure could also be explained.

In comparing our axial line mantle structure with other regions, it is of interest to note that further north along the Afro–Arabian rift system beneath the Afar depression, low uppermost mantle velocities of 7.3–7.7 km/s have been found (Berckhemer et al., 1975) to be underlain by higher velocities of about 8.0 km/s. This velocity structure was determined from a mantle reflection originating at depths of 35–45 km (Makris and Ginzburg, 1987). Progressing further north beneath the Saudi Arabian margin of the southern part of the Red Sea depression, both Prodehl (1985) and Mechie et al. (1986) reported the existence of an upper mantle layer at about 40–45 km depth with a velocity of 8.3–8.4 km/s. However, in this case the Pn velocity exceeded 8.0 km/s although, between the maximum depths to which the Pn penetrated and the high-velocity layer at 40–45 km depth, velocities lower than 7.9 km/s were encountered. Beneath the Jordan–Dead Sea rift system, Ginzburg et al. (1979) reported an upper mantle layer with a velocity of about 8.6 km/s, based on both a mantle reflection and an associated refraction from about 55 km depth. Again in this case, the Pn velocity was about 8.0 km/s.

Good examples of alternating high- and low-velocity layering in the upper mantle include long-offset data from France (Kind, 1974; Ansorge, 1975), from the Early Rise experiment in the U.S.A. (Ansorge, 1975), and from Scandinavia (Cassell and Fuchs, 1979; Stangl, 1990). In the case of the Scandinavian FENNOLORA experiment, Stangl (1990) interpreted the upper mantle layering in terms of petrological compositions and concluded that although the low-velocity layers down to about 170–200 km depths could be explained in terms of isotropic compositions, the high-velocity layers could only be explained in terms of isotropic compositions down to 80–100 km depth. Between depths of about 100 and 200 km, the high-velocity layers required a component of anisotropy.

In summary the low P-wave velocities, less than 7.8 km/s in the uppermost mantle beneath the Kenya rift, can be explained in terms of a few (up to 5) percent of partial melting. The two layers with high velocities in excess of 8.0 km/s identified in the uppermost mantle under the northern part of the rift can be explained in terms of preferred mineral orientation (anisotropy) and in the case of the deeper high-velocity layer basalt depletion may also be required. If olivine is the preferably oriented mineral, then structures with either transverse isotropy or orthorhombic symmetry could result. Horizontal flow, which could be in any azimuth, accompanied by recrystallisation would result in a random orientation of *a*- and *c*-axes of the olivine in the horizontal plane (Nicolas et al., 1971) and would produce a transverse isotropic structure. Horizontal flow along the rift away from the center of a plume situated under the Kenya dome in the southern part of the rift could result in an orthorhombic structure in which 40–55% of the olivine would be required to be preferably oriented in order to explain the high velocities. The process responsible for the flow and the preferred mineral orientation could be shearing near the base of the lithosphere. The north dip on the mantle reflectors is consistent with their representing a complex transition between the lithosphere and the asthenosphere. Thus, the lithosphere would be thinnest under the Kenya dome (Lake Naivasha area) where hot mantle plume material is rising and thermal and magmatic processes are dominant. Here the mantle lithosphere has been thinned much more than the crust (e.g., Morley, 1994). To the north, flowing material may be sinking along the trajectory indicated by the mantle reflectors (Fig. 9). Beneath Lake Turkana in the north, the relative thicknesses of the crust and lithospheric mantle appear consistent with stretching as the dominant process thinning the lithosphere (i.e. an assumed pre-rift lithosphere of 100 km thickness has been thinned to 50 km and an assumed pre-rift crust of 40 km has been thinned to 20 km). This hypothesis needs to be tested by further seismic studies in the Turkana region.

Acknowledgements

Special thanks are due to the Kenya Government for permission to undertake this study. The cooperation and aid of the University of Nairobi, Egerton College, the Department of Mines and Geology, the Ministry of Water Development, and the Survey of Kenya are gratefully acknowledged. This project was financed by grants from the Continental Dynamics Program of the U.S. National Science Foundation, the Science Program of the European Community (EC), and the German Research Society (DFG). IRIS, Inc. assisted with making seismic recorders (SGR's) available. The synthetic seismogram sections were calculated on the Siemens S600 Supercomputer of the computer center at Karlsruhe University. Helpful comments by reviewers are also appreciated.

References

Achauer, U., and the KRISP Teleseismic Working Group, 1994. New ideas on the Kenya rift based on the inversion of the combined data sets of the 1985 and 1989–90 seismic tomography experiments. In: C. Prodehl, G.R. Keller and M.A. Khan (Editors), Crustal and Upper Mantle Structure of the Kenya Rift. Tectonophysics, 236: 305–329.

Ansorge, J., 1975. Die Feinstruktur des obersten Erdmantels unter Europa und dem mittleren Nordamerika. PhD. Thesis. Karlsruhe University.

Ansorge, J. and Mueller, St., 1973. The P-wave structure of the uppermost mantle in Europe based on long-range explosion observations. Z. Geophys., 39: 385–394.

BABEL Working Group, 1990. Evidence for early Proterozoic plate tectonics from seismic reflection profiles in the Baltic shield. Nature, 348: 34–38.

BABEL Working Group, 1991. Recording marine airgun shots at offset between 300 and 700 km. Geophys. Res. Lett., 18: 645–648.

Bamford, D., Jentsch, M. and Prodehl, C., 1979. Pn anisotropy studies in northern Britain and the eastern and western United States. Geophys. J.R. Astron. Soc., 57: 397–429.

Benz, H.M., McCarthy, J. and Mooney, W.D., 1990. Evidence for an upper mantle LVZ and a underlying 80 km-deep discontinuity from the 1987–89 PACE seismic refraction/wide-angle refraction/wide-angle reflection data. Trans. Am. Geophys Union, 71: 1564.

Berckhemer, H., Baier, B., Bartelsen, H., Behle, A., Burkhart, H., Gebrande, H., Makris, J., Menzel, H., Miller, H. and Vees, R., 1975. Deep seismic soundings in the Afar region

and on the highland of Ethiopia. In: A. Pilger and A. Rösler (Editors). Afar Depression in Ethiopia. Schweizerbart, Stuttgart, pp. 89–107.

Burmakov, J.A., Chernyshev, N.M., Vinnik, L.P. and Yegorkin, A.V., 1987. Comparative characteristics of the lithosphere of the Russian platform, the west Siberian platform and the Siberian platform from seismic observations on long-range profiles. Am. Geophys. Union Geodyn. Ser., 17: 175–189.

Cassell, B.R. and Fuchs, K., 1979. Seismic investigations of the subcrustal lithosphere beneath Fennoscandia. J. Geophys., 46: 369–384.

Fuchs, K. and Müller, G., 1971. Computations of synthetic seismograms with the reflectivity method and comparison with observations. Geophys. J.R. Astron. Soc., 23: 417–433.

Fuchs, K. and Vinnik, L.P., 1982. Investigation of the subcrustal lithosphere and asthenosphere by controlled source seismic experiments on long range profiles. Am. Geophys. Union Geodynamics Ser., 8: 81–89.

Fuchs, K., Vinnik, L.P. and Prodehl, C., 1987. Exploring heterogeneities of the continental mantle by high resolution seismic experiments. Am. Geophys. Union Geodyn. Ser., 16: 137–154.

Ginzburg, A., Makris, J, Fuchs, K., Perathoner, B. and Prodehl, C., 1979. Detailed structure of the crust and upper mantle along the Jordan–Dead Sea rift. J. Geophys. Res., 84: 5605–5612.

Guggisberg, B., 1986. Eine zweidimensionale refraktionsseismische Interpretation der Geschwindigkeits–Tiefen-Struktar des oberen Erdmantels unter dem Fennoskandischen Schild (Project FENNOLORA). Ph.D. Nr. 7945, ETH Zürich, 199 pp.

Guggisberg, B., Ansorge, J. and Mueller, St., 1984. Structure of the upper mantle under southern Scandinavia from FENNOLORA data. In: D.A. Galson and St. Mueller (Editors), Proceedings of the First Workshop of the European Geotraverse (EGT) Project—The Northern Segment. Eur. Sci. Found., Strasbourg, pp. 49–52.

Hearn, T.M., 1984. Pn travel times in southern California. J. Geophys. Res., 89: 1843–1855.

Karson, J.A. and Curtis, P.C., 1989. Tectonic and magmatic processes in the eastern branch of the East African rift and implications for magmatically active continental rifts. J. African Earth Sci., 8: 431–453.

Kelly, K.R., Ward, R.W., Treitel, S. and Alford, R.M., 1976. Synthetic seismograms: a finite-difference approach. Geophysics, 41: 2–27.

Kind, R., 1974. Long range propagation of seismic energy to the lower lithosphere. J. Geophys., 40: 189–202.

Macdonald, R., 1994. Petrological evidence regarding the evolution of the Kenya Rift Valley. In: C. Prodehl, G.R. Keller and M.A. Khan (Editors), Crustal and Upper Mantle Structure of the Kenya Rift. Tectonophysics, 236: 373–390.

Maguire, P.K.H., Swain, C.J., Masotti, R. and Khan, M.A., 1994. A crustal and uppermost mantle cross-sectional model of the Kenya Rift derived from seismic and gravity data. In: C. Prodehl, G.R. Keller and M.A. Khan (Editors), Crustal and Upper Mantle Structure of the Kenya Rift. Tectonophysics, 236: 217–249.

Makris, J. and Ginzburg, A., 1987. The Afar Depression: Transition between continental rifting and sea-floor spreading. Tectonophysics, 141: 199–214.

Mechie, J., Prodehl, C. and Koptschalitsch, G., 1986. Ray path interpretation of the crustal structure beneath Saudi Arabia. Tectonophysics, 131: 333–352.

Mechie, J., Keller, G.R., Prodehl, C., Gaciri, S., Braile, L.W., Mooney, W.D., Gajewski, D. and Sandmeier, K.-J., 1994a. Crustal structure beneath the Kenya Rift from axial profile data. In: C. Prodehl, G.R. Keller and M.A. Khan (Editors), Crustal and Upper Mantle Structure of the Kenya Rift. Tectonophysics, 236: 179–199.

Mechie, J., Fuchs, K. and Altherr, R., 1994b. The relationship between seismic velocity, mineral composition and temperature and pressure in the upper mantle—with an application to the Kenya Rift and its eastern flank. In: C. Prodehl, G.R. Keller and M.A. Khan (Editors), Crustal and Upper Mantle Structure of the Kenya Rift. Tectonophysics, 236: 453–464.

Mooney, W.D., Gettings, M.E., Blank, H.R. and Healy, J.H., 1985. Saudi Arabian seismic-refraction profile: a travel-time interpretation of crustal and upper mantle structure. Tectonophysics, 11: 173–246.

Morgan, P., 1983. Constraints on rift thermal processes from heat flow and uplift. In: P. Morgan and B.H. Baker (Editors), Processes of Continental Rifting. Tectonophysics, 94: 277–298.

Morley, C.K., 1994. Interaction of deep and shallow processes in the evolution of the Kenya rift. In: C. Prodehl, G.R. Keller and M.A. Khan (Editors), Crustal and Upper Mantle Structure of the Kenya Rift. Tectonophysics, 236: 81–91.

Nicolas, A., Buchez, J.L., Boudier, F. and Mercier, J.C., 1971. Textures, structures and fabrics due to solid state flow in some European lherzolites. Tectonophysics, 12: 55–86.

O'Reilly, S.Y., Jackson, I. and Bezant, C., 1990. Equilibrium temperature and elastic wave velocities for upper mantle rocks from eastern Australia: implications for the interpretation of seismological models. Tectonophysics, 185: 67–82.

Prodehl, C., 1985, Interpretation of a seismic-refraction survey across the Arabian Shield in western Saudi Arabia. Tectonophysics, 111: 247–282.

Prodehl, C., Jacob, B., Thybo, H., Dindi, E. and Stangl, R., 1994. Crustal structure on the northeastern flank of the Kenya rift. In: C. Prodehl, G.R. Keller and M.A. Khan (Editors), Crustal and Upper Mantle Structure of the Kenya Rift. Tectonophysics, 236: 271–290.

Raitt, R.W., Shor, G.G., Morris, G.B. and Kirk, H.K., 1971. Mantle anisotropy in the Pacific Ocean. Tectonophysics, 12: 173–186.

Rihm, R., Makris, J. and Möller, L., 1991. Seismic surveys in the Northern Red Sea: asymmetric crustal structure. Tectonophysics, 198: 279–295.

Ryaboy, V.Z., 1977. Study of the structure of the lower lithosphere by explosion seismology in the USSR.J. Geophys., 43: 593–610.

Sandmeier, K.-J., 1990, Untersuchung der Ausbreitungseigenschaften seismischer Wellen in geschichteten und streuenden Medien. Ph.D. Thesis, Karlsruhe University.

Slack, P.D. and Davis, P.M., 1994. Attenuation and velocity of P-waves in the mantle beneath the East African Rift, Kenya. In: C. Prodehl, G.R. Keller and M.A. Khan (Editors), Crustal and Upper Mantle Structure of the Kenya Rift. Tectonophysics, 236: 331–358.

Stangl, R., 1990. Die Struktur der Lithosphäre in Schweden abgeleitet aus einer gemeinsamen Interpretation der P- und S-Wellen Registrierungen auf dem FENNOLORA-Profil. Ph.D. Thesis, Karlsruhe University.

Vinnik, L.P. and Ryaboy, V.Z., 1981. Deep structure of the east European platform according to seismic data. Phys. Earth Planet. Inter., 25: 27–37.

Williams, L.A.J., 1972. The Kenya rift volcanics: a note on volumes and chemical composition. Tectonophysics, 15: 83–96.

Yegorkin, A.V. and Pavlenkova, N.I., 1981. Studies of mantle structure of U.S.S.R. territory on long-range seismic profiles. Phys. Earth Planet. Inter., 25: 12–26.